Low frequency sound sources in high-speed turbulent jets

By D. J. Bodony† AND S. K. Lele

1. Motivation and objectives

A gap exists in the understanding of the sources of jet noise and their dependence on external conditions, such as those determined by the nozzle and the environment farther upstream. The influence of nozzle chevrons on the radiated sound is, for example, still characterized parametrically based on a series of experimental studies (Saiyed *et al.* 2003). Further development of an understanding of the "sound sources" in a high-Reynolds-number jet, however, is slowed for two primary reasons: (i) the lack of a universally agreed-upon acoustic theory, and (ii) the difficulty in making experimental measurements suggested by the acoustic theories. The current theories, most notably those of Lighthill (1952), Lilley (1974), Tam & Auriault (1999), and Goldstein (2003) are similar in their arbitrary, but exact, rearrangement of the Navier-Stokes equations (with new variables in the case of Goldstein and a proposed source term by Tam & Auriault), and in the functional form of the identified source term. The acoustic source is of the general form

$$\{\text{linear combination of } \partial_t \text{ and } \partial_{x_i}\}\, S_j(\boldsymbol{x}, t),$$

where the source S_j itself may involve additional differentiation. Measurements of S_j are quite difficult and, currently, only point-measurements of related quantities have been obtained (Panda & Seasholtz 2002; Panda *et al.* 2004). It presently appears that the major practical difference between the dominant theories is in their sensitivity to numerical errors (Freund *et al.* 2005).

Large-eddy and direct numerical computational studies of jet noise offer an alternative to experimental measurements but suffer from the resource requirements imposed by the near-nozzle turbulent annular shear layers for jets at realistic Reynolds numbers. An accurate calculation does not yet exist that includes the nozzle geometry (see, e.g., Andersson *et al.* (2003) and Uzun & Hussaini (2006)) so most studies have concentrated on the portion of the jet immediately downstream of the nozzle exit plane (Freund 2001; Bogey *et al.* 2003; Bodony & Lele 2004, 2005). (A review of the use of large-eddy simulations (LES) for jet noise prediction is given in Bodony & Lele (2006).) The direct numerical simulation (DNS) of Freund (2001) continues to be the only calculation of its type; post-processing of the DNS data has been useful in evaluating key assumptions (e.g., Khavaran *et al.* (2002)). However, the high cost, low Reynolds number, and single jet operating point of the DNS calculation are limiting.

To complement the DNS calculation of Freund and to develop and expand the capabilities of LES for jet noise prediction, a series of numerical simulations were conducted by the authors for jets at six operating conditions with Mach numbers ranging from 0.4 to 2.0 of both heated and unheated jets. Details of the calculations are available in Bodony

† Present address: Department of Aerospace Engineering, University of Illinois at Urbana-Champaign

& Lele (2005). Due to resolution limitations the far-field sound of the simulations is limited to those frequencies with $St = fD_j/U_j \leq 1.2$; near-field frequencies are limited to $St \leq 1.5$.

This paper is concerned with those jets originally presented in Bodony & Lele (2005) having $M_j \geq 0.9$, which includes two unheated jets and one heated jet. Additional analysis is performed on the databases generated by the space-time histories of the jets to investigate characteristics of the sound generation. To do so we adopt Lighthill's acoustic analogy (Lighthill 1952) and explore its ability to predict the sound of the jets as compared to the sound directly captured in the compressible LES calculations. Effects of jet Mach number and temperature on the radiated sound, in the context of Lighthill's theory, are discussed.

1.1. *Objectives*

Using the LES databases described in Bodony & Lele (2005) the objectives of this work are to critically examine the ability of Lighthill's acoustic analogy to predict the acoustic spectra of hot and cold high-speed jets. To accomplish this we first present a comparison of the Lighthill-predicted sound spectra to the directly computed sound spectra from the compressible LES calculations. We then examine in more detail the components of the Lighthill spectra.

2. Sound predictions using Lighthill's theory

2.1. *Previous work*

Lighthill's theory has been used previously in numerical noise prediction. For a plane (2-D) jet Bastin *et al.* (1997) found that the monopole source form $S = \partial_{x_i}\partial_{x_j}T_{ij}$, where

$$T_{ij} = \rho u_i u_j + [(p - p_\infty) - a_\infty^2(\rho - \rho_\infty)]\delta_{ij} - \tau_{ij} \tag{2.1}$$

is the Lighthill stress tensor, yielded inferior sound predictions relative to the alternative far-field expression involving $\ddot{T}_{ij}$ or its counterpart in the freqency domain, which are in appropriate quadrupole forms. In his round jet Freund (2001) found using the identity

$$S = \frac{\partial^2}{\partial t^2}(\rho - \rho_\infty) - a_\infty^2 \frac{\partial^2}{\partial x_j \partial x_j}(\rho - \rho_\infty), \tag{2.2}$$

that noise predictions using Lighthill's theory compared well with the instantaneous pressure time history. Later Freund (2002) showed that the Lighthill-predicted noise spectrum at $\Theta = 30^\circ$ compared well with the DNS data and with the data of Stromberg *et al.* (1980). Freund also discussed the relative roles of the "shear noise," "self noise," and "entropy" terms embedded in T_{ij}.

2.2. *Frequency domain considerations*

In this section we use the space-time databases generated from the simulations to demonstrate the feasibility of using LES in combination with Lighthill's theory to predict jet noise and to extend the predictions to heated jets.

The calculation of the far-field sound using Lighthill's theory begins by considering the integral form of the time-Fourier-transformed version of Eq. 2.2,

$$\widehat{\rho - \rho_\infty}(\boldsymbol{x};\omega) := \widehat{\rho'}(\boldsymbol{x};\omega) = \frac{1}{4\pi a_\infty^2} \int_{\mathcal{R}^3} \frac{e^{i\omega R/a_\infty}}{R} \hat{S}(\boldsymbol{y};\omega)\, \mathrm{d}\boldsymbol{y}, \tag{2.3}$$

where $R = |\boldsymbol{x} - \boldsymbol{y}|$ and $\hat{S}$ is the transformed monopole source. The advantage of using the frequency-domain form of Eq. 2.3 and not its time-domain analog is in avoiding the interpolation needed for the evaluation of S at the retarded time $t - R/a_\infty$. An alternative form that follows from integrating Eq. 2.3 by parts twice (and assuming the boundary terms vanish for a surface taken to infinity) is

$$\widehat{\rho'}(\boldsymbol{x};\omega) = \frac{1}{4\pi a_\infty^2} \int\limits_{\mathcal{R}^3} \frac{\partial^2}{\partial y_i \partial y_j} \left\{ \frac{e^{i\omega R/a_\infty}}{R} \right\} \hat{T}_{ij}(\boldsymbol{y};\omega)\, \mathrm{d}\boldsymbol{y} \tag{2.4}$$

where the quadrupole Fourier amplitude $\hat{T}_{ij}$ now appears explicitly.

In view of Eq. 2.1 the resultant density Fourier amplitudes can be considered as the sum of the components

$$\widehat{\rho'}_{\mathrm{tot}} = \widehat{\rho'}_{\mathrm{mom}} + \widehat{\rho'}_{\mathrm{ent}} + \widehat{\rho'}_{\mathrm{vis}},$$

where

$$\widehat{\rho'}_{\mathrm{mom}}(\boldsymbol{x};\omega) = \frac{1}{4\pi a_\infty^2} \int\limits_{\mathcal{R}^3} \frac{\partial^2}{\partial y_i \partial y_j} \left\{ \frac{e^{i\omega R/a_\infty}}{R} \right\} \widehat{\rho u_i u_j}(\boldsymbol{y};\omega)\, \mathrm{d}\boldsymbol{y}, \tag{2.5}$$

$$\widehat{\rho'}_{\mathrm{ent}}(\boldsymbol{x};\omega) = \frac{1}{4\pi a_\infty^2} \int\limits_{\mathcal{R}^3} \frac{\partial^2}{\partial y_j \partial y_j} \left\{ \frac{e^{i\omega R/a_\infty}}{R} \right\} \left(\widehat{p'} - a_\infty^2 \widehat{\rho'} \right)(\boldsymbol{y};\omega)\, \mathrm{d}\boldsymbol{y}, \tag{2.6}$$

and

$$\widehat{\rho'}_{\mathrm{vis}}(\boldsymbol{x};\omega) = \frac{-1}{4\pi a_\infty^2} \int\limits_{\mathcal{R}^3} \frac{\partial^2}{\partial y_i \partial y_j} \left\{ \frac{e^{i\omega R/a_\infty}}{R} \right\} \widehat{\tau}_{ij}(\boldsymbol{y};\omega)\, \mathrm{d}\boldsymbol{y}. \tag{2.7}$$

Freund (2003) found that the viscous stress contribution to $\hat{T}_{ij}$ was negligible; hence, we take $\widehat{\rho'}_{\mathrm{vis}} \equiv 0$. We also do not consider the the contribution of the subgrid scale (SGS) stresses to the Lighthill-determined acoustic spectra and focus solely on the sound due to the resolved field.

3. Observations

Application of the integral form of Lighthill's analogy (Eq. 2.4), for the Mach 0.9 unheated jet is shown for the two observer angles of 30° and 90° at a distance of $30D_j$ in fig. 1. The Kirchhoff surface predictions for the same jet at the corresponding angles are also shown for comparison. There is reasonable agreement at both angles within the statistical uncertainty due to the limited LES data record length. The peak SPL (sound pressure level) and the corresponding peak frequency are captured in the Lighthill integrations. (Freund (2003), for the 30° prediction, saw similar agreement with his DNS database.) Similar spectral shapes are seen in both prediction methods at each angle.

In fig. 2 the Lighthill and Kirchhoff surface predictions are repeated for the Mach 2 unheated jet. As with the near-sonic cold jet the two sound predictions are similar for a wide range of Strouhal numbers. The peak SPL and Strouhal number are captured as is the spectral shape for all frequencies. At 30° the Lighthill-predicted spectrum is 2 dB below the Kirchhoff spectrum for $0.4 \leq St \leq 1.0$. As $St \to 1.5$, the predictions begin to differ due to grid resolution limitations with the Lighthill prediction being the higher. Our Kirchhoff surface data are not reliable beyond $St = 1.2$ for this jet.

The Mach 1 heated jet results are shown in fig. 3 where, again, the two methods yield similar predictions over a range of frequencies. For both angles the Lighthill prediction

shows an over prediction for $St < 0.2$, although the Kirchhoff surface data shows increased oscillations in SPL at these frequencies, indicative of the limited statistical sample. The peak frequency appears to be closer to $St = 0.2$ at this operating condition for each angle.

For each jet the contributions to the total spectrum by the momentum term (Eq. 2.5) and the so-called entropy term (Eq. 2.6) are presented next. The decomposition due to Lilley (1974) of

$$p - p_\infty - a_\infty^2(\rho - \rho_\infty) := p' - a_\infty^2\rho' = \underbrace{-\frac{\gamma-1}{2}\rho u_k u_k}_{\text{term I}} + \underbrace{a_\infty^2 \int \frac{\partial}{\partial x_k}\left[\rho u_k \left(\frac{h_\infty - h_s}{h_\infty}\right)\right] \mathrm{d}t}_{\text{term II}}, \tag{3.1}$$

with h_∞ and h_s being the freestream and static enthapies, is used to further examine the spectra. Such a decomposition was also used by Freund (2003) for his Mach 0.9 jet. Note that term II involves an integral over time but may be related to the local total energy via the energy equation.

Figure 4 shows the decomposition for the unheated Mach 0.9 jet. At 30° and at 90° the momentum contribution dominates the overall spectrum; for the shallower angle it over-contributes by approximately 2 dB (as also found by Freund (2003)). The $p' - a_\infty^2\rho'$ contribution is a relatively small portion in an overall SPL sense, approximately 10 dB below the momentum term's level. However, for frequencies $St < 1$ at $\Theta = 30°$, there is some cancellation between $\rho u_i u_j$ and $p' - a_\infty^2\rho'$. It is interesting to note that at low frequencies, at 30°, the entropic (term II) contribution to $p' - a_\infty^2\rho'$ is minimal but increases with increasing frequency. At 90° the momentum term dominates at all frequencies and shows very little, if any, correlation with $p' - a_\infty^2\rho'$ for the available range of frequencies. At 30° there is significant interplay between the entropy components term I and term II, especially at higher frequencies.

For the Mach 2 cold jet (fig. 5) at 30° the Lighthill-predicted spectra are of a different nature than for the Mach 0.9 cold jet; at 90° the high-speed jet spectra is qualitatively the same as for the lower speed jet. Figure 5(a) shows that (i) there is much greater $(\rho u_i u_j)$—$(p' - a_\infty^2\rho')$ cancellation at all frequencies, and (ii) the peak frequency of the individual spectra near $St = 1$ does not correspond to the peak frequency of the total spectrum's peak of $St = 0.3$. (There does, however, appear to be a weak local maximum near $St = 0.3$ for the individual spectra.) Below $St = 0.4$ the momentum stress term is approximately 3 dB greater than the total SPL, indicating cancellation. For this range of frequencies ($St < 0.4$) we find that term I $\gg$ term II for the entropy contribution; at higher frequencies they are of comparable magnitude. At $St = 0.4$ and above, the $\rho u_i u_j$ and $(p' - a_\infty^2\rho')\delta_{ij}$ contributions become increasingly anticorrelated to yield a total SPL that is much less than the individual SPLs. Conversely, for $St \geq 0.4$, the term I and term II portions of $p' - a_\infty^2\rho'$ show constructive interference.

Turning to the 90° spectrum in fig. 5(b) we find that it is the momentum stress that is the dominant source of the radiated noise. The so-called entropy term contributes very little at all frequencies. The spectral peak occurs near $St = 0.3$ for all individual spectra and for the total spectrum.

When the Mach 1 heated jet, with $T_j/T_\infty = 2.3$, is considered as in fig. 6, we find a picture that differs in some important aspects from the unheated jet at the same velocity. At 30° the heated jet's component spectra show a St peak well beyond the peak frequency of the total spectrum, although there is a minor local maximum near $St = 0.2$

in the individual spectra. Over all frequencies the $\rho u_i u_j$ and $p' - a_\infty^2 \rho'$ contributions are closely correlated, especially at higher frequencies; it is now the term II component that is most important. Indeed, $-[(\gamma - 1)/2]\rho u_k u_k$ seems to play a very small role. At 90° the momentum and term II components combine constructively for the total SPL for $St < 0.4$ but add destructively for higher frequencies. At both angles the decay of the total SPL with increasing St shows a different functional form than do the individual spectra.

4. Discussion

The aforementioned observations highlight additional aspects of the Lighthill-predicted sound spectra that are worth discussing in greater detail. The first is the difference in the 30° individual component spectra and the total spectrum for the high-speed jets as shown in figures 5(a) and 6(a). The second is the amount of cancellation that occurs for the high-speed jets between the momentum and entropic contributions.

4.1. *High-speed jet spectra at* $\Theta = 30°$ *and* 90°

The Mach 2.0 unheated and Mach 1.0 heated jets exhibit qualitatively different spectra at 30° for the *individual* components of $\hat{T}_{ij}$ compared to its sum, in contrast to the Mach 0.9 cold jet as found here (fig. 4) and earlier by Freund (2003). To examine the cause consider the further decomposition of the momentum term $\rho u_i u_j$ into

$$\rho u_i u_j = \overline{\rho}\,\overline{u}_i\overline{u}_j + \underbrace{\overline{\rho}(\overline{u}_i u_j' + u_i'\overline{u}_j)}_{L_1} + \underbrace{\rho'\overline{u}_i\overline{u}_j}_{L_2} + \underbrace{\rho'(\overline{u}_i u_j' + u_i'\overline{u}_j)}_{Q_1} + \underbrace{\overline{\rho}u_i'u_j'}_{Q_2} + \underbrace{\rho' u_i' u_j'}_{C} \tag{4.1}$$

where an overbar denotes a time-averaged quantity with corresponding fluctuation denoted by the prime. The terms L_1 and L_2 are linear in the fluctuations; Q_1 and Q_2 are quadratic in the fluctuations; and C is cubic. The very first term, $\overline{\rho}\,\overline{u}_i\overline{u}_j$, has only a mean component and does not radiate sound; it is not considered further. The spectra for the five remaining terms are plotted in fig. 7 for the Mach 2 cold jet and in fig. 8 for the Mach 1 heated jet. From the figures it is apparent that the subcomponents of $\rho u_i u_j$ are qualitatively similar to the overall $\rho u_i u_j$ spectrum.

For the Mach 2.0 cold jet in the 30° direction, the cubic term is of the least importance at all frequencies. The linear term $L_2 = \rho'\overline{u}_i\overline{u}_j$ is of the most importance for $St \geq 0.5$ while L_1 dominates for $St < 0.5$. At 90° the linear term L_2 becomes of the least importance at all frequenices while the two terms $L_1 = \overline{\rho}(\overline{u}_i u_j' + u_i'\overline{u}_j)$ and $Q_2 = \rho'(\overline{u}_i u_j' + u_i'\overline{u}_j)$ contribute most to the overall spectrum, with the latter term dominating for $St < 0.5$. It is notable that the linear term L_2 swaps dominance completely with the pair (L_1, Q_2) when the observer angle is changed.

For the Mach 1.0 heated jet (fig. 8) we find the linear term L_2 dominates at all frequencies, with the quadratic term Q_2 being within 5 dB over the spectrum. The linear term L_1 is confined to $St \leq 0.1$, while the terms Q_1 and C are 8–10 dB and 10–15 dB, respectively, below the L_2 contribution. At 90° the linear term L_2 is far below the overall spectrum and does not appear on the scale of fig. 8(b). For all frequencies the Q_1 quadratic term accounts for the majority of the overall $\rho u_i u_j$ spectrum, while the spectra of L_1 and C are similar but does not appear to contribute to the total.

Historically those terms proportional to $\overline{u}_i$, i.e., those that include the mean velocity, have been associated with the notion of "shear noise" (Goldstein 1976), where the sound is generated by the interaction of fluctuations with the mean flow. Another interpretation

is that the sound is redistributed by the mean flow through refraction. For the case of $L_2 = \rho'\overline{u}_i\overline{u}_j$ for the 30° observer the significant cancellation that occurs with the term $(p' - a_\infty^2\rho')$ suggests that neither of these two interpretations are appropriate; if they were appropriate one would not expect such a large portion of the available energy to be non-radiating.

The linearity of L_2 in the density fluctuations implies that the portion of the far-field density spectrum due to L_2 will be proportional to $\omega^4 S_{\rho\rho}$ in the Fraunhaufer limit, where $S_{\rho\rho}$ is the spectrum of ρ',

$$S_{\rho\rho} = \int \langle \rho'(t)\rho'(t+\tau)\rangle \exp\{i\omega\tau\}\,\mathrm{d}\tau.$$

For weakly compressible turbulence it is expected that $\rho'/\overline{\rho} \sim (u'/\overline{a})^2$ and, similarly, $p'/\overline{p} \sim (u'/\overline{a})^2$. Thus $S_{\rho\rho} \sim S_{uu}S_{uu}$ functionally so that the density and pressure fluctuation spectra are, to leading order in $u'/\overline{a}$, quadratic in the velocity spectra. For the 30° observer, then, the term $\rho'\overline{u}_x\overline{u}_x$ dominates the six terms of L_2 and has a frequency dependence that is functionally similar to Q_2, the term quadratic in the velocity fluctuations. Near-field temporal spectra of ρ' and u_x' (not shown, but available in Bodony (2004)) demonstrate that this is indeed the case.

Finally, we note that for the Mach 0.9 unheated jet, the lower mean shear and consequently lower fluctuation root-mean-square (rms) values are not able to produce meaningful levels of ρ' (Bodony & Lele 2005) to be of consequence in the sound radiated to the far-field.

The dominance of the L_2 term for the 30° observer for both the Mach 2.0 cold and Mach 1.0 hot jets then explains the strong correlation of $\rho u_i u_j$ with $(p' - a_\infty^2\rho')\delta_{ij}$. Because $\overline{u}_x \sim a_\infty$ in the sound generating portion of the jet (Bodony & Lele 2005) and because $\rho u_i u_j \approx \rho'\overline{u}_x\overline{u}_x\delta_{ij}$, we have the leading two terms canceling, leaving $p'\delta_{ij}$ and the remaining terms of $\rho u_i u_j$, all of which are of lower magnitude.

At 90° the relevance of the L_2 is lowered as the radial mean velocity component $\overline{u}_r$ is very small relative to $\overline{u}_x$ and a_∞ in the radiating portion of the jet. The terms $L_1 \approx \overline{\rho}\,\overline{u}_x u_r'$, $Q_1 \approx \overline{\rho}\,\overline{u}_x u_r'$, and $Q_2 = \overline{\rho}u_i'u_j'$ thus remain possible contributors to the overall sound radiation. For the heated jet, with its low value of mean density in the sound-generating region, $L_{1,\mathrm{hot}} < L_{1,\mathrm{cold}}$ given that the velocity fluctuation levels are very similar in magnitude between the cold and hot jets. For the cold jet at 90° we thus expect $L_1 > Q_1, Q_2$, which is observed for $St \geq 0.5$ while at lower frequencies $Q_2 > L_1$. For the heated jet at 90° the observation angle and low mean density imply that $Q_2 > Q_1, L_1$.

We note that the ordering arguments are made based on order-of-magnitude estimates and do not consider the frequency dependence of the fluctuations, other than the ω^2 contribution coming from the Green's function.

4.2. *On Lilley's decomposition of T_{ij}*

From observations of the unheated jets at 90° it appears that both constituents of the $p' - a_\infty^2\rho'$ term, namely term I and term II as defined in Eq. 3.1, are of approximately equal magnitude and combine to form the "entropic" contribution to the SPL. For the heated jet, however, it is the enthalpy fluctuation term that takes precedence. This and the fact that, for the unheated jets at least, some cancellation occurs between the $\rho u_i u_j$ and $[(\gamma-1)/2]\rho u_k u_k$ terms suggest that it may be more useful to prefer the decomposition

(Lilley 1974) of

$$T_{ij} = \underbrace{\rho u_i u_j - \frac{\gamma - 1}{2}\rho u_k u_k \delta_{ij}}_{\text{momentum stress}} + \underbrace{a_\infty^2 \int \frac{\partial}{\partial x_k}\left[\rho u_k \left(\frac{h_\infty - h_s}{h_\infty}\right)\right]\delta_{ij}\,\mathrm{d}t}_{\text{enthalpy flux}} \underbrace{-\tau_{ij}}_{\text{viscous stress}} \tag{4.2}$$

to better describe the roles of the various stresses to the sound spectra. The presence of the integral in time implies a non-local dependence of the sound field on the enthalpy fluxes. However, through the energy equation it is possible to write

$$\int \frac{\partial}{\partial x_k}\left[\rho u_k \left(\frac{h_\infty - h_s}{h_\infty}\right)\right]\,\mathrm{d}t$$

as $\rho(E/h_\infty - 1)$, where E is the total energy per unit mass, so that the appearance of the time integral is not unphysical. In using Eq. 4.2 the independence in modeling of the momentum and enthalpy fluctuations may be helpful. This conclusion is further borne out by the relative roles played by the momentum and "entropy" terms for the hot Mach 1 jet.

At 30° the data suggest that Lilley's decomposition may also be beneficial. It was discussed previously that the leading terms of $\rho u_i u_j$ and $(p' - a_\infty^2 \rho')\delta_{ij}$ almost completely cancel for the high-speed jets considered in this study. In Lilley's rearrangement of T_{ij} this cancellation occurs naturally within the momentum stress term, leaving the enthalpy flux contribution and the remaining momentum stress terms. As the arguments made in determining the canceling are general, we would expect this conclusion to hold for other, high-speed jets with $U_j \geq a_\infty$ up to those jets with $M_j > 2.5$ where Mach wave radiation becomes important.

5. Conclusions

Based upon the investigation of the space-time databases provided by three large-eddy simulations of high-speed turbulent jets, the accuracy of Lighthill's acoustic analogy has been examined. It was found that the Lighthill predictions agreed very well with the directly computed radiated sound for jets of Mach numbers 0.9 (cold), 1.0 (hot), and 2.0 (cold). Investigation of the sound spectra showed that the momentum contribution due to $\rho u_i u_j$ was dominant at 90° but its overall effect was dependent on cancellation with the so-called entropy component $p - p_\infty - a_\infty^2(\rho - \rho_\infty)$ at 30°. In the cold Mach 0.9 jet the momentum stress was the determining factor for the sound spectra; at higher jet velocities this contribution was tempered by the $-[(\gamma - 1)/2]\rho u_k u_k \delta_{ij}$ portion of the entropy term for the cold jet and by the "enthalpy flux" term for the heated jet. Modeling of the sound sources is believed to be made easier by considering the combined term $\rho u_i u_j - [(\gamma - 1)/2]\rho u_k u_k \delta_{ij}$ separate from the enthalpy flux, due to Lilley (1974), as the latter term is more important for heated jets. At 30° it does not appear that considering the momentum and entropic portions of T_{ij}, in its original Lighthill (1952), is entirely beneficial, as the leading order contributions from these two terms cancel. That high-speed jets are quieter when heated (keeping the jet velocity constant) appears to be due to a reduced sound-generating volume and a reduced convective jet Mach number.

6. Acknowledgements

This work was partially funded by the Aeroacoustics Research Consortium and by the Center for Turbulence Research. Computer resources were provided by the Department of Defense through contract AFOSR F49620-01-1-0138. The authors thank Professor J. Freund of the University of Illinois at Urbana-Champaign for access to his data. An earlier, limited version of this article appeared as AIAA paper AIAA-2005-3041 and was presented at the AIAA/CEAS Aeroacoustics Conference and Exhibit in Monterey, California, 22–25 May 2005.

REFERENCES

Andersson, N., Eriksson, L.-E. & Davidson, L. 2003 Large-Eddy Simulation of a Mach 0.75 Jet. AIAA Paper 2003-3312, Presented at the 9th AIAA/CEAS Aeroacoustics Conference and Exhbit, Hilton Head, S.C., 12–14 May.

Bastin, F., Lafon, P. & Candel, S. 1997 Computation of jet mixing noise due to coherent structures: plane jet case. *J. Fluid Mech.* **335**, 261–304.

Bodony, D. J. 2004 Aeroacoustics of Turbulent Free Shear Flows. PhD thesis, Stanford University, Stanford, California.

Bodony, D. J. & Lele, S. K. 2004 Jet noise prediction of cold and hot subsonic jets using large-eddy simulation. AIAA Paper 2004-3022, Presented at the 10th AIAA/-CEAS Aeroacoustics Conference, Manchester, U.K., May 10–12.

Bodony, D. J. & Lele, S. K. 2005 On using large-eddy simulation for the prediction of noise from cold and heated turbulent jets. *Phys. Fluids* **17** (085103).

Bodony, D. J. & Lele, S. K. 2006 Review of the current status of jet noise predictions using large-eddy simulation (invited). AIAA Paper 2006-0468, Presented at the 44th Aerospace Sciences Meeting and Exhibit, Reno, NV.

Bogey, C., Bailly, C. & Juvé, D. 2003 Noise investigation of a high subsonic, moderate Reynolds number jet using a compressible LES. *Theor. Comp. Fluid. Dyn.* **16**, 273–297.

Freund, J. B. 2001 Noise sources in a low-Reynolds-number turbulent jet at Mach 0.9. *J. Fluid Mech.* **438**, 277–305.

Freund, J. B. 2002 Turbulent jet noise: Shear noise, self-noise, and entropic contributions. AIAA Paper 2002-2423, Presented at the 8th AIAA/CEAS Aeroacoustics Conference & Exhibit, Breckenridge, C.O., 17–19 June.

Freund, J. B. 2003 Noise-source turbulence statistics and the noise from a Mach 0.9 jet. *Phys. Fluids* **15** (6), 1788–1799.

Freund, J. B., Samanta, A., Wei, M. & Lele, S. K. 2005 The robustness of acoustic analogies. AIAA Paper 2005-2940, Presented at the 11th AIAA/CEAS Aeroacoustics Conference and Exhibit, Monterey, CA, 23–25 May.

Goldstein, M. E. 1976 *Aeroacoustics*. New York, N. Y.: McGraw-Hill.

Goldstein, M. E. 2003 A generalized acoustic analogy. *J. Fluid Mech.* **488**, 315–333.

Khavaran, A., Bridges, J. & Freund, J. B. 2002 A Parametric Study of Fine-Scale Turbulence Mixing Noise. AIAA Paper 2002-2419, Presented at the 8th AIAA/-CEAS Aeroacoustics Conference, June 17–19, 2002, Breckenridge, Colorado.

Lighthill, M. J. 1952 On sound generated aerodynamically I. General theory. *Proc. R. Soc. London A* **211**, 564–587.

Lilley, G. M. 1974 On the noise from jets. *Tech. Rep.* AGARD CP-131.

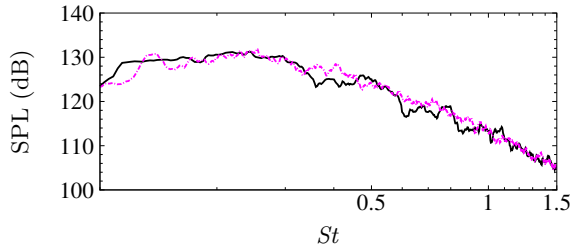

(a) $\Theta = 30^\circ$

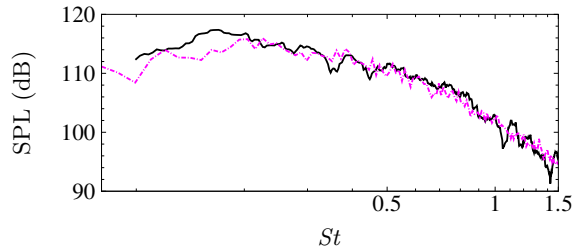

(b) $\Theta = 90^\circ$

FIGURE 1. Narrowband spectra at $\mathcal{R} = 30D_j$ for the Mach 0.9 unheated jet M09TR086. Legend: −, Lighthill (total), – · –, Kirchhoff Surface.

PANDA, J. & SEASHOLTZ, R. G. 2002 Experimental investigation of density fluctuations in high-speed jets and correlation with generated noise. *J. Fluid Mech.* **450**, 97–130.

PANDA, J., SEASHOLTZ, R. G., ELAM, K. A., MIELKE, A. F. & ECK, D. G. 2004 Effect of heating on turbulent density fluctuations and noise generation from high speed jets. AIAA Paper 2004-3016, Presented at the 10th AIAA/CEAS Aeroacoustics Conference & Exhibit, Manchester, U.K., 10–12 May.

SAIYED, N. H., MIKKELSEN, K. L. & BRIDGES, J. E. 2003 Acoustics and Thrust of Quiet Separate-Flow High-Bypass-Ratio Nozzles. *AIAA J.* **41** (3), 372–378.

STROMBERG, J. L., MCLAUGHLIN, D. K. & TROUTT, T. R. 1980 Flow field and acoustic properties of a Mach number 0.9 jet at a low Reynolds number. *J. Sound Vib.* **72**, 159–176.

TAM, C. K. W. & AURIAULT, L. 1999 Jet Mixing Noise from Fine-Scale Turbulence. *AIAA J.* **37** (2), 145–153.

UZUN, A. & HUSSAINI, M. 2006 High Frequency Noise Generation in the Near-Nozzle Region of a Jet. AIAA Paper 2006-2499, Presented at the 12th AIAA/CEAS Aeroacoustics Conference and Exhibit, Cambridge, MA.

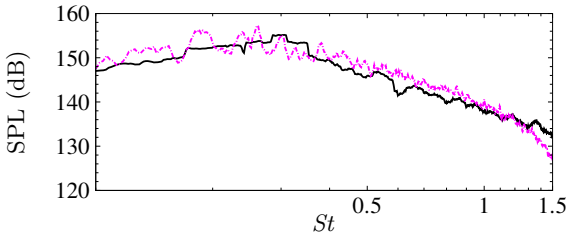

(a) $\Theta = 30^\circ$

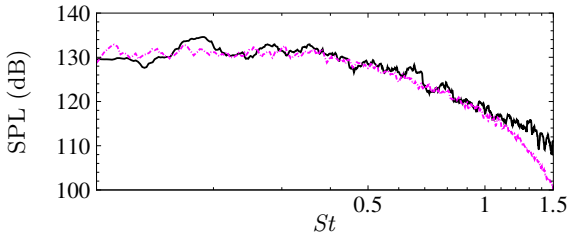

(b) $\Theta = 90^\circ$

FIGURE 2. Narrowband spectra at $\mathcal{R} = 30D_j$ for the Mach 2.0 unheated jet M15TR056. Legend: $-$, Lighthill (total), $-\cdot-$, Kirchhoff Surface.

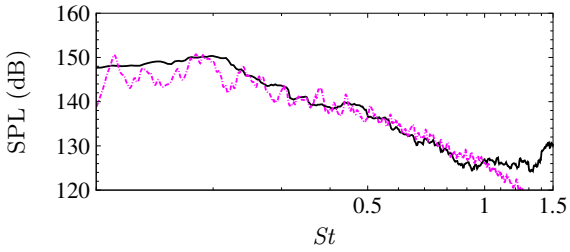

(a) $\Theta = 30^\circ$

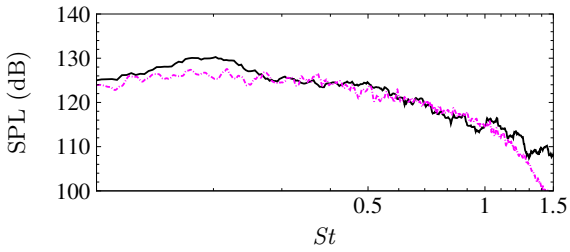

(b) $\Theta = 90^\circ$

FIGURE 3. Narrowband spectra at $\mathcal{R} = 30D_j$ for the Mach 1.0 heated jet M15TR230. Legend: $-$, Lighthill (total), $-\cdot-$, Kirchhoff Surface.

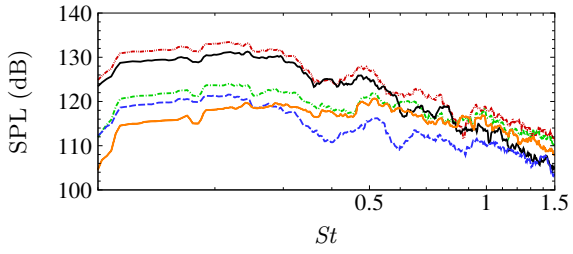

(a) $\Theta = 30^\circ$

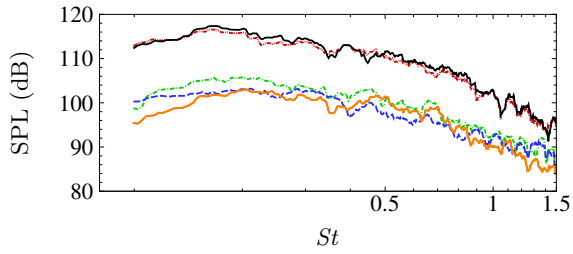

(b) $\Theta = 90^\circ$

FIGURE 4. Narrowband spectra at $\mathcal{R} = 30D_j$ for the Mach 0.9 unheated jet M09TR086. Legend: −, total, − · ·−, $\rho u_i u_j$, − · −, $p' - a_\infty^2 \rho'$, − −, entropy (term I), · · ·, entropy (term II).

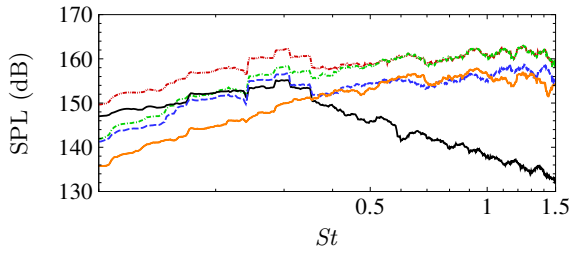

(a) $\Theta = 30^\circ$

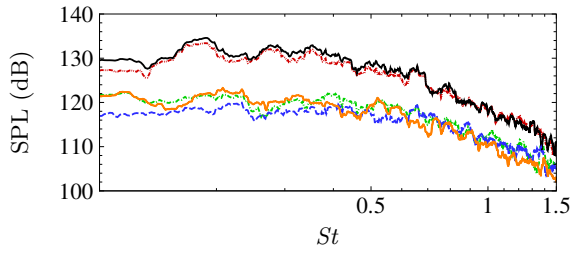

(b) $\Theta = 90^\circ$

FIGURE 5. Narrowband spectra at $\mathcal{R} = 30D_j$ for the Mach 2.0 unheated jet M15TR056. Legend: −, total, − · ·−, $\rho u_i u_j$, − · −, $p' - a_\infty^2 \rho'$, − −, entropy (term I), · · ·, entropy (term II).

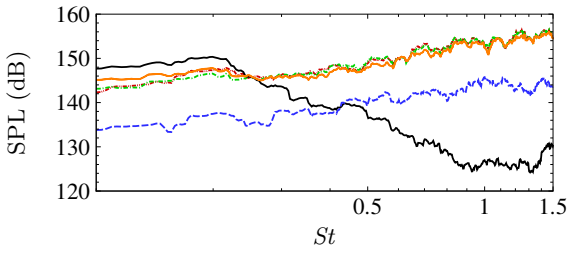

(a) $\Theta = 30°$

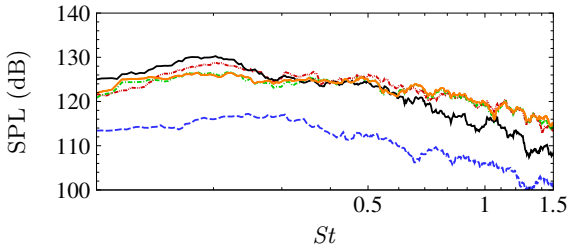

(b) $\Theta = 90°$

FIGURE 6. Narrowband spectra at $\mathcal{R} = 30D_j$ for the Mach 1.0 heated jet M15TR230. Legend: —, total, — · · —, $\rho u_i u_j$, — · —, $p' - a_\infty^2 \rho'$, – –, entropy (term I), · · ·, entropy (term II).

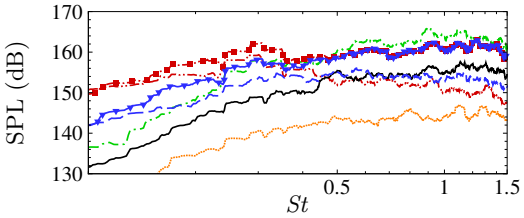

(a) $\Theta = 30°$

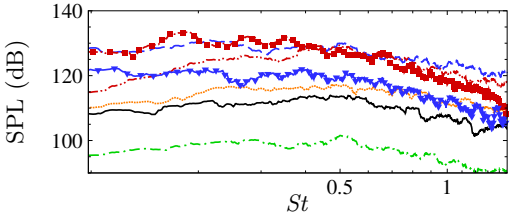

(b) $\Theta = 90°$

FIGURE 7. Component spectra contributing to the spectrum of $\rho u_i u_j$ for the jet M15TR056. Legend: — · · —, L_1; — · —, L_2; —, Q_1; – –, Q_2; · · · , C; —▼—, $p' - a_\infty^2 \rho'$; —■—, $\rho u_i u_j$ spectrum.

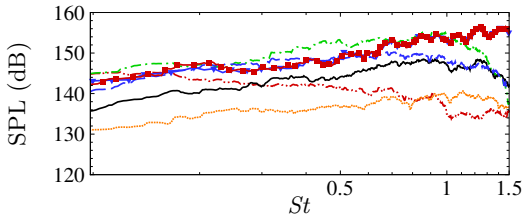

(a) $\Theta = 30^\circ$

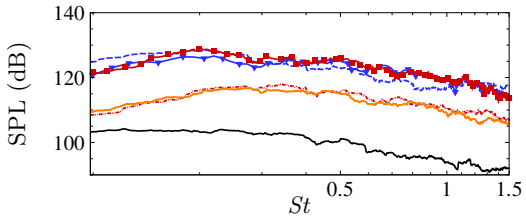

(b) $\Theta = 90^\circ$

FIGURE 8. Component spectra contributing to the spectrum of $\rho u_i u_j$ for the jet M15TR230. Legend: $- \cdot\cdot -, L_1$; $- \cdot -, L_2$; —, Q_1; $- -, Q_2$; $\cdots, C$; $-\blacktriangledown-$, $p' - a_\infty^2 \rho'$; $-\blacksquare-$, $\rho u_i u_j$ spectrum. Note the curve for L_2 in (b) lies below the figure scale.